LAWRENCE
LIVERMORE
NATIONAL
LABORATORY

LLNL-JRNL-408767

Thermal and Mechanical Design Aspects of the LIFE Engine

R. P. Abbott, M. A. Gerhard, J. F. Latkowski, K. J. Kramer, K. R. Morris, P. F. Peterson, J. E. Seifried

November 17, 2008

Fusion Science and Technology

Disclaimer

THERMAL AND MECHANICAL DESIGN ASPECTS OF THE LIFE ENGINE

Ryan P. Abbott[1], Michael A. Gerhard[1], Jeffery F. Latkowski[1], Kevin J. Kramer[1,2], Kevin R. Morris[1], Per F. Peterson[2], and Jeffrey E. Seifried[2]

[1]*Lawrence Livermore National Laboratory, Livermore, CA, 94550, abbott13@llnl.gov*
[2]*University of California, Berkeley, CA, 94720*

The Laser Inertial confinement fusion - Fission Energy (LIFE) engine encompasses the components of a LIFE power plant responsible for converting the thermal energy of fusion and fission reactions into electricity. The design and integration of these components must satisfy a challenging set of requirements driven by nuclear, thermal, geometric, structural, and materials considerations. This paper details a self-consistent configuration for the LIFE engine along with the methods and technologies selected to meet these stringent requirements. Included is discussion of plant layout, coolant flow dynamics, fuel temperatures, expected structural stresses, power cycle efficiencies, and first wall survival threats. Further research and to understand and resolve outstanding issues is also outlined.

I. INTRODUCTION

The fundamental enabling idea behind a LIFE power plant is the coupling of a laser driven inertial fusion neutron source to a subcritical fission blanket to achieve *in-situ* fuel production, power multiplication, and deep burn (Ref. 1). This hybrid approach overcomes fundamental limitations of each technology yielding a system with several advantages over what either could achieve alone. Key among these advantages are a relaxed fusion development pathway, a reduction in the proliferation concerns and repository requirements that plague pure fission, and an ability to directly access vast stores of energy present in stockpiles of fertile material such as depleted uranium.

The major components of a LIFE power plant include a factory for fabricating fusion targets, a laser driver to ignite them, a central chamber where the fusion pulses take place and the fission fuel is housed, a power conversion system, tritium storage units, and a fuel inspection facility. Fig. 1 illustrates the layout of these major components along with the structures that house them.

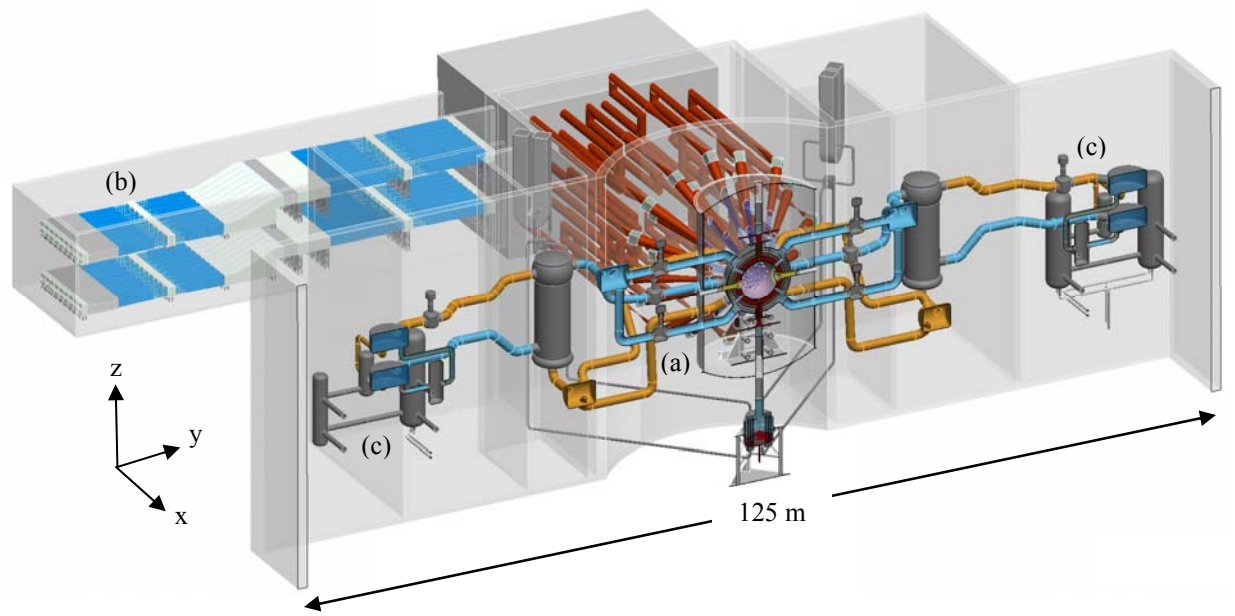

Fig. 1. A view of the LIFE power plant with (a) central chamber, (b) laser driver, and (c) power conversion systems.

This paper focuses on the systems required to convert the thermal output of the fusion and fission reactions into electrical power. Collectively these components are called the LIFE engine and the following sections survey the various nuclear, thermal, structural, and material considerations that have led to its current design.

While several variations exist for a LIFE power plant, for the purposes of discussion this paper assumes a particular configuration employing 37.5 MJ target yields ignited at 13.3 Hz by a NIF-like hotspot target illumination geometry for 500 MW of fusion. The total power is 2.0 GW_{th}.

II. PLANT LAYOUT

A LIFE power plant consists of six major regions. External to the main structure that houses most other systems is the laser driver. There are many possible options for the laser system depending on the chosen target ignition method. Depicted in Fig. 1 is a driver for central hot-spot ignited targets using an indirect-drive illumination geometry like that used in the National Ignition Facility (NIF). Other options include low solid-angle hot-spot ignition and low solid-angle fast ignition layouts.

While x-axis of the main structure is devoted to laser beam routing, the y-axis is occupied by the two power conversion systems connected to the central chamber. A level up, that same axis of the building houses a high bay to facilitate maintenance and periodic chamber replacement. Below the central vacuum vessel and chamber sits a pebble dump tank to where fuel is relocated in the event of a loss of coolant accident.

The quadrants of the main structure diagonal to the laser and power cycles axes house a fusion target production factory, pebble inspection facilities, primary coolant processing equipment, and tritium storage beds; none of which are yet integrated into the plant layout.

III. CENTRAL CHAMBER

The central chamber is the heart of a LIFE engine where lasers ignite fusion targets, their neutrons are multiplied and moderated, fissile fuel and tritium is produced, and thermal energy is transferred to the primary coolant. Fuel, beryllium multiplier, and carbon reflector pebbles along with first wall and primary coolant must all get in and out of the system while allowing the passage of 48 laser beams and injected fusion targets. Because the central chamber houses so many processes and serves so many functions its design is challenging.

III.A. Radial Build

The LIFE central chamber is segregated into several functional radial regions by a series of spherical shells which will be made from high-temperature, radiation resistant steel.[†] Beam and coolant injection tubes, along with additional ribbing members, tie the various shells to each other as well as to the outer wall from which they and all the contents of the central chamber ultimately suspend. Fig. 2 shows a model of a LIFE central chamber illustrating this radial structure.

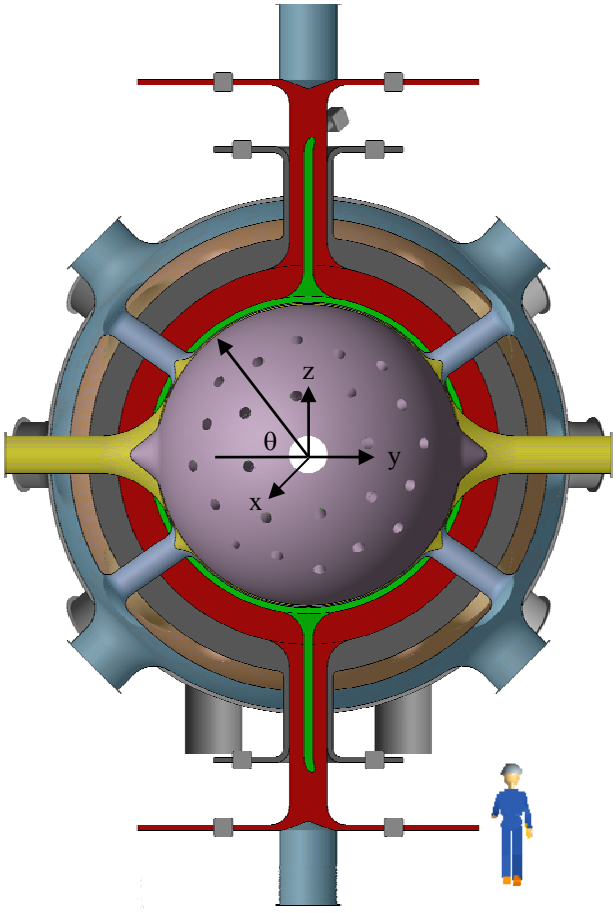

Fig. 2. The inner structure of the LIFE central chamber.

III.A.1. Central Cavity

The innermost region of the central chamber is a cavity 2.5 m in radius into which the fusion targets are injected and then ignited by 48 laser beams using a NIF-like illumination geometry. A background of xenon gas at 4 μg/cm^3 (1.8×10^{16} atoms/cm^3) is maintained in

[†] The mechanical properties of the oxide dispersion strengthened (ODS) ferritc steel composition 12YWT are currently assumed for design purposes.

this region to protect the first wall from target emitted ions and x-rays. This gas density is sufficient to stop virtually all the ions and attenuate 80-90% of the x-rays while allowing 90% transmission of the 350 nm ('3ω') driver beams (Ref. 2). After a fusion pulse, the resulting plasma cools and vents through the beam tubes until conditions return to their pre-shot state and the cycle repeats.

II.A.2. First Wall Cooling and Stress

The first wall is made from a 2.75 mm thick shell of ODS steel which has a 250 μm coating of tungsten on its inner surface. This refractory armor protects the first wall from the pulsed temperature spikes induced primarily by target emitted x-rays that penetrate the background gas in the central cavity. Calculations with the RadHeat code (Ref. 3) predict a temperature pulse of 950 K as shown in Fig. 3. While the compressive thermal stress induced from these pulses will exceed the yield strength of the tungsten coating, experiments and analyses performed as a part of the HAPL program indicate that the resulting stress-relieving cracks will not propagate to the steel substrate (Ref. 4).

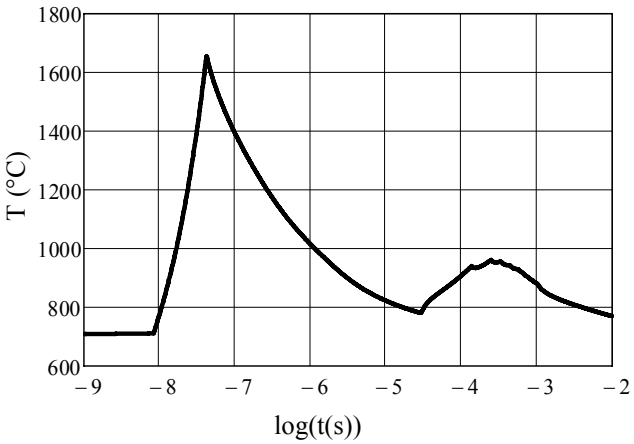

Fig. 3. Transient temperature response of the first wall inner surface as a function of time.

It has been conservatively assumed that all the energy initially present in the target emitted x-rays and ions will be radiated to the first wall either immediately or as the central cavity plasma cools. With 22% (12% x-rays + 10% ions) of the 500 MW fusion power in this form and a first wall volumetric nuclear [neutron (n) + γ-ray] heating of 24 W/cm^3, a heat flux totaling 1.46 MW/m^2 must ultimately be conducted through the first wall. Because the ODS steel has a thermal conductivity of ≈ 25 W/m/K, this heat flux will impose a steady state temperature gradient of 50 K/mm through the first wall driving the inner surface to ≈ 140 K hotter than the outer surface.

Keeping the first wall ODS steel below a chosen temperature limit of 700 °C requires vigorous dedicated cooling. The Pb-Li eutectic (83% Pb + 17% Li) has been chosen for this as, in addition to having excellent heat transfer properties, it serves as a neutron multiplier and tritium breeder. With a mass flow rate of 4.6 MT/s, this coolant enters the central chamber at 260 °C along the y-axis (see Fig. 2) via a single 50 cm diameter tube. The coolant flows from this tube into a 3 cm gap behind the first wall where convection coefficients of up to 35 kW/m^2/K are achieved. Fig. 4 shows the Pb-Li, first wall outer surface, and first wall inner surface temperatures as a function of the polar angle position shown in Fig. 2.

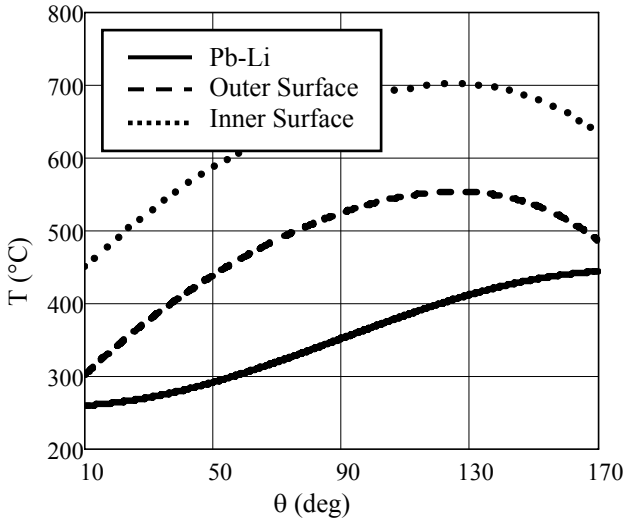

Fig. 4. Temperatures for first-wall coolant, outer, and inner surfaces as a function of polar angle position.

The 50 K/mm steady state temperature gradient will lead to a compressive thermal stress of 150 MPa on the first wall's inner surface and a tensile stress of 200 MPa on its outer surface. The transient temperature response will result in additional 30 MPa tensile stress pulses on the outside surface as is shown in Fig. 5. Taken alone these stresses could represent potential rupture or fatigue threats. A comprehensive first wall threat assessment must, however, include structural stresses, which may counter the tensile thermal stresses discussed above. Section III.B discusses 3D calculations being performed to compose a complete stress field for the first wall.

III.A.3. Flibe Inner Injection Plenum

While first wall cooling requires a liquid with a relatively low melting point and viscosity to keep it within temperature limits, the rest of the central chamber is cooled with the molten salt flibe (2 LiF + BeF_2), which

is a factor of five less dense but has 2.5 times the volumetric heat capacity. In order to supply the coolest flibe to the most vigorously heated fuel while minimizing pressure drops and structural loads the coolant is injected into a plenum below the multiplier, fuel, and reflector layers and allowed to flow radially outward through these regions.

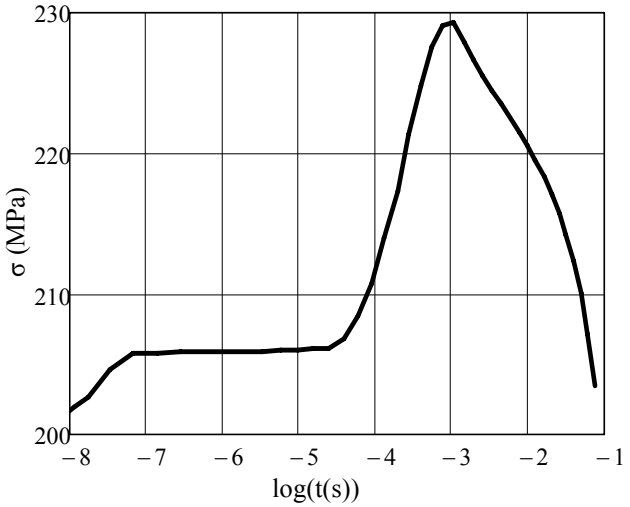

Fig. 5. Transient thermal stress response of the first wall outer surface as a function of time.

The inner injection plenum is a 3 cm gap supplied at with flibe 24 MT/s via 24 internal tubes having a 50 cm diameter. They are distributed evenly to produce an isotropic radial flow pattern. To minimize the number of external connections that must be made during chamber replacement, these tubes are connected to an outer injection plenum which is supplied by eight 100 cm diameter tubes. To allow for the radial flow of flibe, the multiplier, fuel, and reflector regions are bounded by 3 mm thick ODS steel shells that are 25% perforated and do not impose a significant impedance.

III.A.4. Neutron Multiplier

The neutron multiplier zone is a 16 cm thick region filled by 1 cm diameter beryllium pebbles randomly packed at 60%. Swelling due to helium production from $^{9}Be + n \rightarrow 2\alpha + 2n$ reactions requires these pebbles be removed from the central chamber for heat treatment and recompaction annually. With a density of 1.85 g/cm^3 these pebbles are buoyant in flibe and are, therefore, injected at the bottom of the chamber and extracted at the top. There will be approximately 15 million beryllium pebbles in a 5.0 m inner diameter LIFE central chamber.

The average volumetric nuclear heating (n + γ–ray) in this region is 17 W/cm^3. The flibe coolant will flow outward through this region at a superficial speed of 15 cm/s and achieve heat transfer coefficients of approximately 10 kW/m^2/K. The flibe coolant exits this region at 615 °C and the beryllium pebbles are held to temperatures of 620 °C.

III.A.5. Fuel

The nominal LIFE fuel form assumed for nuclear analysis is 1 mm diameter TRISO particles formed into 2 cm diameter spherical pebbles with a 70% carbon matrix. Fifteen million of these fuel pebbles packed at 60% fill this radial region, which extends from 273 to 360 cm in radius. Fig. 6 shows the volumetric nuclear heating in the fuel region as a function of radial position. As the flibe slows to ≈ 10 cm/s as a result of an increase in flow cross sectional area, heat transfer coefficients drop to ≈ 7 kW/m^2/K. The innermost pebbles experience the highest temperatures with surfaces and center-points at 700 °C and 820 °C, respectively. The flibe enters this region at 615 °C and exits at 640 °C. Because they have a nominal density of 2.43 g/cm^3, which is greater than flibe's 2.0 g/cm^3, the fuel pebbles are injected at the top of the chamber and flow downward for extraction.

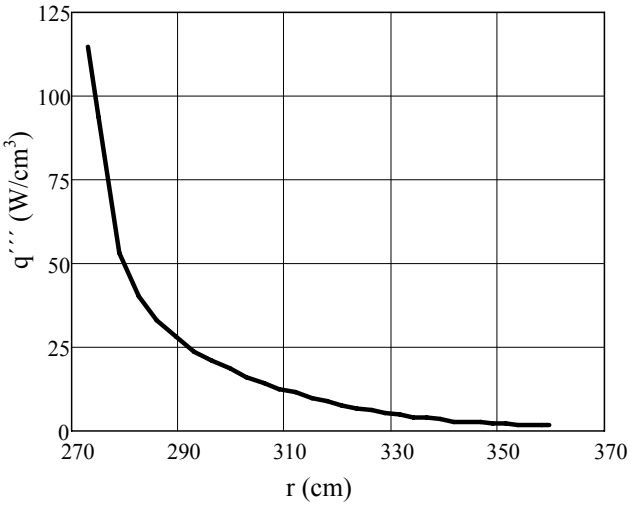

Fig. 6. Nuclear heating profile in the LIFE fuel region.

As all the fission product energy will be deposited in the fuel kernels at the center of each TRISO particle, they will experience a temperature and thermal stress pulse after every fusion target ignites. Neutronic calculations indicate that the energy deposition process will take about 20 μs. Fig. 7 shows the results transient simulations determining the radial and hoop stresses seen by the silicon carbide in the TRISO particle which occur just after all the fission energy has been deposited and the fuel kernel has spiked in temperature by 65 K. The radial build of the TRISO particle modeled is given in Table 1.

As can be seen, the 100 μm thick silicon carbide (SiC) layer at the outside of the particle sees a peak tensile hoop stress of approximately 60 MPa which is ≈ 20% of SiC's 270 MPa tensile strength at 800 °C (Ref. 5).

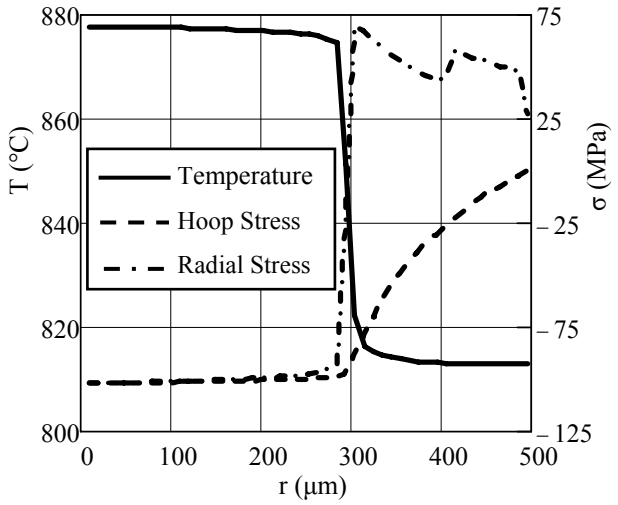

Fig. 7. Fuel kernel temperature and thermal stress profiles at 20 μs after fuel kernel temperature pulse.

TABLE I. TRISO particle radial build.

r (μm)	0 - 300	300 - 402	402 - 407	407 - 497
material	UCO	Buffer-PyC	PyC	SiC

III.A.6. Reflector

The reflector region is 75 cm thick and resides just outside the fuel region. It is also filled with 2 cm diameter pebbles at 60% packing but composed of pure graphite. The flibe moving through this region slows to ≈ 6 cm/s. There will be about 20 million reflector pebbles. Because the reflector region experiences a relatively low volumetric heating of < 1 W/cm^3, any temperature fluctuations in the coolant as a result of unsteady non-isotropic flow in the fuel region is smoothed out. This homogenization is important for protecting the extraction tubes from thermal shock.

It will likely be beneficial to control the fuel-to-moderator ratio as the fissile composition of the fuel pebbles changes over time. To accomplish this it is possible to exchange reflector and fuel pebbles between the two regions. To match the fuel pebble density the reflector pebbles will be impregnated with tungsten ballast at 1.4% by volume.

III.A.7. Flibe Extraction Plenum

After passing through the reflector pebble bed the flibe transits a final 3 mm thick perforated shell into a 15 cm thick flibe extraction plenum. The flibe then flows into eight 100 cm diameter tubes to deliver its thermal energy to the two power conversion systems**.** The total pressure drop for the flibe coolant as it passes through the multiplier, fuel, and reflector pebble beds is relatively modest at ≈ 50 kPa. While this pressure differential is a significant source of structural loading on the solid internal chamber structures, consideration of the forces imposed by the coolant and pebble bed hydrostatic pressures must also be taken into account when determining an overall static structural stress state for the central chamber.

III.B. Structural Stresses

The flow and gravity driven hydraulic pressures exerted on the various solid chamber structures by the two coolant liquids and the multiplier, fuel, and reflector pebble beds will result in steady-state stress field. This field must be quantified to ensure the central chamber will not yield, buckle, or deform unacceptably from thermal creep during its operational lifetime of between four and eight years. Additionally, the dynamic response of the central chamber to the pulsed heating and pressurization of the Pb-Li, flibe, and solid chamber structures must be evaluated to determine if there are any significant fracture or fatigue threats.

III.B.1 Static Structural Stresses

A static structural model of the LIFE central chamber has been constructed with the NIKE3D code (Ref. 6). It includes all of the solid chamber structures such as region partitions, beam ports, and coolant injection tubes. Loads on these structures from the coolants and pebble beds are calculated analytically and imposed manually. Results of analyses conducted with this model will drive the design of a detailed ribbing layout which is compatible with all coolant and pebble flows while ensuring the central chamber will exhibit substantial safety factors from failure due to yield, creep rupture, or buckling. Fig. 8. is a representative stress plot generated from the model demonstrating that stress concentration points near beam tubes are the only areas where structural stress magnitudes approach 100 MPa; a factor of more than two below 12YWT's 5 year, 700 °C creep rupture strength of 225 MPa (Ref. 7).

III.B.2. Dynamic Loading

It is also recognized that dynamic structural loading from pulsed isochoric heating of the coolant and chamber needs to be evaluated. One-dimensional models in DYNA3D (Ref. 8) are currently being composed to assess the magnitude of the potential threat. If dynamic effects cannot be neglected, eventually detailed two and three-

dimensional models will be constructed with additional ribbing and other reinforcement added as necessary.

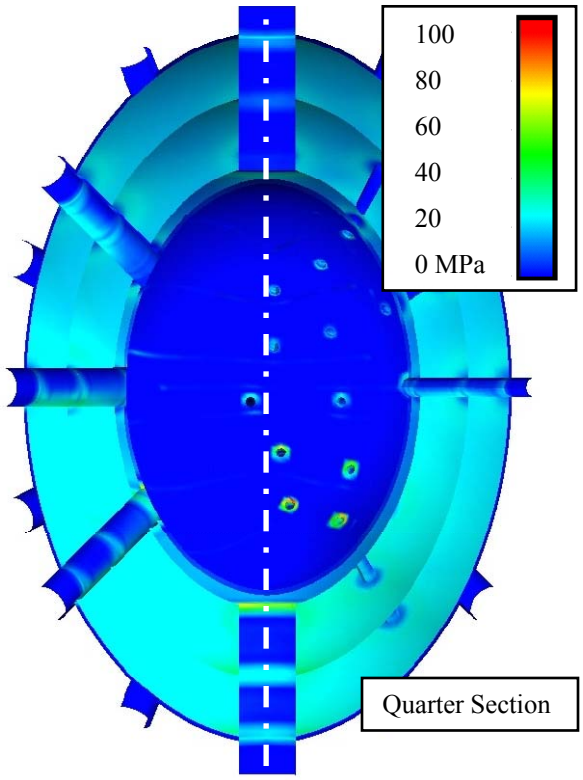

Fig. 8. A stress field plot for the LIFE central chamber.

IV. POWER SYSTEMS

LIFE power plants will employ a multiple-reheat helium Brayton power cycle to convert thermal energy into electricity. Zhao and Peterson (Ref. 9) state that the higher power densities these systems can achieve will result in a smaller footprint and lower capital costs than comparable steam Rankine cycles. Equally important, the use of an inert gas working fluid eliminates any threat of chemical reactions with the molten salt coolant and avoids having tritiated water in the system.

The current 3ω hot-spot ignition LIFE power plant design uses two identical power conversion systems located symmetrically on either side of the central chamber along the y-axis (as shown in Fig. 1) to simplify pipe routing and provide redundancy. The flibe primary coolant transfers its thermal energy to a flinak secondary loop. Flinak is a significantly less expensive molten salt but with comparable volumetric heat capacity to flibe. This intermediate loop is coupled to the helium loop via compact heat exchangers which serve as the reheaters in the Brayton cycle. Each independent power cycle has a 1000 MW_{th} capacity and at LIFE's primary coolant outlet temperature of 640 °C achieves a conversion efficiency of approximately 43% assuming typical turbine and compressor efficiencies. With an estimated coolant pumping power of 20 MW and a laser recirculating power of 175 MW the net electric output is 665 MW. Greater power outputs are possible if any combination of larger target yields, faster ignition rates, higher blanket gains, or greater thermal efficiencies are realized or employed.

Using supercritical CO_2 is a possible alternative to helium in the power cycle. The compression work is reduced using a fluid near the critical point so compressor and turbine equipment can be smaller (Ref. 10). However, a supercritical CO_2 system will necessarily run at greater pressures (20 vs. 10 MPa) and there may be material corrosion issues associated with using a non-inert working fluid (Ref. 9).

V. PERIODIC MAINTENANCE

Even with ODS steel's estimated dispersion stability of between 150 and 300 dpa (Ref. 10), with a damage rate of 35 dpa/yr the central chamber will need to be replaced every four to eight years. The layout of the LIFE power plant has been designed to facilitate this change out and minimize the required plant downtime.

Before a central chamber can be replaced its multiplier, fuel, and reflector pebbles will need to be removed to storage tanks. Those for the fuel pebbles will require the ability to passively remove the fission product decay heat. Normally, all the fuel pebbles will cycle through the system every 30 to 60 days for inspection but when a chamber replacement is planned, removal can be accelerated to a few days with the LIFE engine producing reduced power while the system empties.

The LIFE power plant layout currently includes a large high bay running along the y-axis of the main building just above the power conversion systems. A large gantry crane will remove the lid of the vacuum chamber housing the central chamber thus allowing access to the various coolant pipes that will need to be disconnected robotically. Once all disconnections are made the crane can lift the old central chamber from its support pedestal to a temporary rest in the high bay. The new chamber can then be placed, coolant and pebble piping connections re-established and the vacuum chamber re-sealed. After refueling the new chamber and establishing active cooling the fusion systems can be activated and normal operations resumed.

VI. OUTSTANDING ISSUES AND FUTURE WORK

Because the LIFE power plant is pulsed system, volumetric heating of the coolant and chamber structures will occur isochorically. The dynamic response of the

central chamber to this pressurization will need to be studied in detail and its design modified if any significant fracture or fatigue threats are uncovered. Additionally, the dynamics of pebble flow need to be investigated both computationally and experimentally to determine if radial stratification can be maintained, which will allow system designers to tailor the fuel burn characteristics by preferentially placing particular pebbles in higher or lower neutron flux regions. Detailed time and motion studied need to be completed to determine the time required for chamber replacement and its potential impact on plant capacity factors.

VII. CONCLUSIONS

While far from complete, the LIFE power plant design now self consistently integrates several major subsystems and necessary servicing procedures. The central chamber is structured to maintain the necessary radial configuration of neutron multiplier, fuel, and reflector pebbles while allowing for target injection, proper laser illumination, and coolant flows. It is able to support the structural loads due to the hydrostatic and hydrodynamic pressures of the coolant and pebble beds while exhibiting stresses well within the material limits at the chosen operating temperatures. The plant layout facilitates a streamlined chamber replacement strategy to minimize downtime and maximize capacity factors. The helium Brayton power cycle achieves high thermal conversion efficiencies with a reduced footprint compared to equivalently sized steam Rankine systems.

ACKNOWLEDGMENTS

This work performed under the auspices of the U.S. Department of Energy by Lawrence Livermore National Laboratory under Contract DE-AC52-07NA27344.

REFERENCES

1. K. J. KRAMER et al., “Neutron Transport and Nuclear Burnup Analysis for the Laser Inertial Confinement Fusion-Fission Energy (LIFE) Engine,” *Fusion Science and Technology*, submitted (2008).
2. S. C. WILKS et al., “Beam Propagation for LIFE,” *Fusion Science and Technology*, submitted (2008).
3. R. P. ABBOTT, "RadHeat v2.4 User's Manual," UCRL-SM-237324 (2007).
4. J. P. BLANCHARD and R. RAFFRAY, "Laser Fusion Chamber Design," *Fusion Science and Technology*, **52**, 440 (2007).
5. L. L. SNEAD, “Handbook of SiC Properties for Fuel Performance Modeling,” *Journal of Nuclear Materials*, **371**, 347 (2007).
6. B. N. MAKER, "NIKE3D A Nonlinear, Implicit, Three-Dimensional Finite Element Code For Solid and Structural Mechanics User's Manual," UCRL-MA-105268 Rev. 1 (1995).
7. R. L. KLUEH et al., “Tensile and Creep Properties of an Oxide Disperson-Strenghtened Ferritic Steel,” *Journal of Nuclear Materials*, **307-311**, 773 (2002).
8. J. I. LIU, "DYNA3D: A Nonlinear, Explicit, Three-Dimensional Finite Element Code for Solid and Structural Mechanics User Manual," UCRL-MA-107254 (2005).
9. H. ZHAO and P. F. PETERSON, "Optimization of Advanced High-Temperature Brayton Cycles with Multiple-Reheat Stages," *Nuclear Technology*, **158**, 145 (2007).
10. V. DOSTAL et al., “The Supercritical Carbon Dioxide Power Cycle: Comparison to Other Advanced Power Cycles,” *Nuclear Technology*, **154**, 283 (2006).
11. T. R. ALLEN et al., "The Stability of 9Cr-ODS Oxide Particles Under Heavy-Ion Irradiation," *Nuclear Science and Engineering*, **151**, 305 (2005).